

結 語

Soap bubble MIP処理によりsegmental stenosisをより明確に描出することが可能となった。

文 献

- 1) 昭和58年度厚生省“川崎病に関する研究”班：川崎病による冠動脈障害診断の基準化に関する小委員会答申（班長：川崎富作，小委員会委員長：神谷哲郎）。
- 2) Etienne A, Botnar RM, Van Muiswinkel AM, et al : “Soap-Bubble” visualization and quantitative analysis of 3D coronary magnetic resonance angiograms. Magn Reson Med 2002 ; 48 : 658-666.
- 3) Takemura A, Suzuki A, Inaba R, et al : Utility of coronary MR angiography in children with Kawasaki disease. AJR Am J Roentgenol 2007 ; 188 : W534-W539.
- 4) Weber OM, Martin AJ, Higgins CB : Whole-heart steady-state free precession coronary artery magnetic resonance angiography. Magn Reson Med 2003 ; 50 : 1223-1228.
- 5) Suzuki A, Kamiya T, Ono Y, et al : Clinical significance of morphologic classification of coronary arterial segmental stenosis due to Kawasaki disease. Am J Cardiol 1993 ; 71 : 1169-1173.
- 6) 勝又康行, 鈴木淳子, 武村 濃ほか : MRCA coronary angiographyにおける再疎通血管の描出と心筋障害の評価. Prog Med 2007 ; 27 : 1574-1578.
- 7) Suzuki A, Takemura A, Inaba R et al : Magnetic resonance coronary angiography to evaluate coronary arterial lesions in patients with Kawasaki disease. Cardiol Young 2006 ; 16 : 563-571.
- 8) Nagel E, Klein C, Paetsch I, et al : Magnetic resonance perfusion measurements for the noninvasive detection of coronary artery disease. Circulation 2003 ; 108 : 432-437.
- 9) 稲葉利佳子, 鈴木淳子, 佐藤克彦ほか : 川崎病冠動脈障害の描出における3次元Magnetic Resonance Coronary Angiographyの有用性. 日小児会誌 2002 ; 106 : 1636-1641.
- 10) 武村 濃, 鈴木淳子, 稲葉利佳子ほか : 川崎病冠動脈障害に対するMR coronary vessel wall imagingの検討. Prog Med 2005 ; 25 : 1833-1836.
- 11) 岩井光弘, 立石敏樹, 武田聡司ほか : Whole Heart MRCAにおける撮像時間短縮の検討—スライス厚の評価. 北海道放線技誌 2005 ; 65 : 19-25.

Detection of Coronary Arterial Segmental Stenosis due to Kawasaki Disease by Magnetic Resonance Coronary Angiography Using Soap Bubble Maximum Intensity Projection

Atsushi Takemura¹⁾, Atsuko Suzuki²⁾, Tsutomu Kitazume²⁾,
Tomoyoshi Sonobe³⁾, Keiji Tsuchiya³⁾ and Tateo Korenaga¹⁾

- 1) Department of Radiology, Tokyo Postal Services Agency Hospital
- 2) Department of Pediatrics, Tokyo Postal Services Agency Hospital
- 3) Department of Pediatrics, Japanese Red Cross Medical Center

臨床化学的・免疫学的検査所見

小川 俊一

Biochemical and immunological laboratory findings in Kawasaki disease

Shunichi Ogawa

Department of Pediatrics, Nippon Medical School

Abstract

There is no specific diagnostic test for Kawasaki disease, but certain laboratory findings are characteristics. In acute phase of Kawasaki disease, neutrophils with toxic granules, CRP, ESR are elevated. The platelet count is generally normal in the 1st week of illness and rapidly increases by the 2nd-3rd week of illness. The hepatic transaminases, total cholesterol, LDL, and total bilirubin are increased in the acute stage. On the other hand, total protein, albumin and sodium are generally decreased during 1st-2nd week of illness. Sterile pyuria and cerebrospinal fluid pleocytosis may be present. Moreover, the cytokines, the growth factors, and the adhesion molecules are elevated according to the intensity of vasculitis.

Key words: Kawasaki disease, biochemical findings, immunological findings

はじめに

川崎病の発見より40年以上が経過した。この間に血液・生化学的な一般検査所見においては新たな発見はない。一方、血液中のサイトカイン、細胞増殖因子、接着因子、各種バイオマーカーなどには次々に新たな知見がもたらされている。

本稿では主として最近の臨床化学的、免疫学的検査所見について概説する。

1. 従来的一般検査所見

a. 血液一般

一般的に病初期は幼若好中球の増加を主体とする白血球の増多が認められる。約半数は

15,000/ μ l以上となる。赤血球、血色素量およびヘマトクリットは病初期より軽度の低下が認められる症例が多く、病2-3週でより顕著となることがある。血小板は病初期には正常範囲内のことが多いが、血小板数が減少している症例があり、そのような症例では冠動脈瘤を合併する可能性が高く、冠動脈瘤合併のリスクファクターとなる。一方、病2-3週に血小板数はピークとなり、しばしば数カ月後にまで及ぶこともある。また、血小板数の増加は100万/ μ l以上になることもある。更に血小板機能も亢進する。好中球の増多や中毒顆粒が認められること、血小板の増多にはIL-6(interleukin-6), IL-8, G-CSF(granulocyte colony-stimulating factor), M-CSF(monocyte colony-stimulating factor)

などの関与が考えられている。

b. CRP, 血沈

最近では血沈ではなく CRP 値が臨床上主に用いられる。CRP の増加は主として TNF- α (tumor necrosis factor- α) や IL-6 などのサイトカインによる肝細胞での産生能の亢進による。CRP 値は病初期より高値を呈し、臨床症状の改善に伴い急速に低下する。CRP 値も冠動脈瘤合併のリスクファクターとなる。

c. 生化学

1) 血清総蛋白, アルブミン

血清総蛋白は病初期よりほとんどが正常ないしは軽度低下し、 γ グロブリン製剤の使用により増加する。一方、血清アルブミンは血管炎に伴う血管透過性の亢進、IL-6 による肝での合成能の低下などにより低下する。血清アルブミン値も冠動脈瘤合併のリスクファクターである。

2) 血清トランスアミナーゼ

血清トランスアミナーゼは病初期に GOT, GPT ともに 50 IU/l 以上を示す症例が多い。ただし、500 IU/l を凌駕する症例はまれであり、多くは第 2-3 週で正常化する。更に、直接ビリルビン, LAP, γ -GTP などの上昇をみる。直接ビリルビンの増加は胆嚢腫大やサイトカインによる肝細胞における胆汁酸の取り込み障害や、細胆管への分泌障害のためと考えられている。

3) 血清電解質

血清電解質では重症例において Na の低下が認められる。低 Na 血症も冠動脈瘤合併のリスクファクターとなる。

4) 脂質代謝

脂質代謝では病初期より総コレステロール値および HDL (high density lipoprotein cholesterol) が低下し、LDL (low density lipoprotein cholesterol) が増加する。川崎病の急性期では M-CSF の増加に伴いマクロファージが大量に血中に動員されその結果、脂質代謝異常を来し総コレステロール, HDL を低下させている¹⁾。最近になり、単球/マクロファージ由来のケモカインである MCP-1 (monocyte-chemoattractant protein-1) やその受容体である CCR-2 の発現の増加、更に血管炎に伴い増加する iNOS などは、遠隔期

において晩期障害として動脈硬化の初期段階への進行に関与する可能性が示唆されている²⁾。

5) 溶連菌の関与

川崎病への溶連菌の関与は現在のところ、定かではないが、溶連菌抗体価である抗ストレプトリジン O (ASO) は一般に低値であり、高値を示す症例はまれである。

d. 免疫グロブリン, 補体, 抗核抗体

病初期には IgG, IgM, IgA, IgE すべてが高値を呈する³⁾。更に、 γ グロブリンによる治療のために IgG は著明に増加する。特に、冠動脈の拡張や瘤形成が認められた症例では IgG および IgM の有意な増加が認められている⁴⁾。なお、回復期にはすべての免疫グロブリンは正常に復する。

補体についてみると C3 は発症後より 1-3 週間は高値を呈し、その後、正常に復する。C4 および CH50 は経過を通じて有意な変動はない³⁾。また、抗核抗体には有意な上昇は認められない。

e. 尿・髄液所見

病初期に軽度の蛋白尿と無菌性膿尿が認められる症例が多いが、蛋白尿は熱性と思われる。また、膿尿は無菌性の尿路感染によるものと考えられている。更に、髄液においても軽度の細胞増多が認められるが、髄膜の血管炎に伴う一過性のものと考えられている。

2. 新たな臨床化学的検査所見

ルーチンの検査としては施行されることは少ないが、最近の医学の進歩により病因、病態、予後を考えるうえで重要な因子が同定され臨床に供されつつある。

a. サイトカインの変動

川崎病の急性期にはほとんどの炎症性サイトカインが上昇し、血管炎の発症、増悪に深くかかわっている。炎症性サイトカインは単球/マクロファージ, Tリンパ球, 血管内皮細胞, 線維芽細胞などから産生されるが、主に単球/マクロファージ, Tリンパ球などの免疫担当細胞の活性化に伴うとされ、特に川崎病における血管炎では単球/マクロファージの活性化に伴う

ものが大きいとされている。川崎病におけるサイトカインについては別稿で詳細に記述されているので本稿では詳細については割愛する。サイトカインの中でもTNF- α , IL-1, IL-6, IL-8, MCP-1, G-CSF, M-CSFなどのサイトカインが病初期に増加する。これらは血球上での発現が亢進するだけでなく、病初期には血清中においても有意に増加し、血管炎の形成、およびその後の血管障害に大きくかかわる⁵⁻¹²⁾。一般的に急性期に増加していたサイトカインの多くは γ グロブリン大量療法により減少する。川崎病の急性期においてはTNF- α , IL-1, IL-6の発現の上昇、血清レベルでの増加に伴い血管内皮細胞を刺激し、接着因子であるICAM-1 (intercellular adhesion molecule-1), VCAM-1 (vascular cell adhesion molecule-1), E-selectinなどの発現を増加させ、主として単球の血管内皮細胞への接着に関与し、血管炎の発症、進展を助長している^{5,13,14)}。

b. 血管作動性物質の変動

川崎病において血管作動性物質は急性期から遠隔期における、血管炎、血管再構築、血栓形成、血管新生、動脈硬化などの病態に深くかかわっている。

1) 急性期における血管作動性物質の動態

a) 血管弛緩・血小板凝集抑制・細胞増殖抑制作用因子

血管拡張性ペプチドとしては一酸化窒素 (nitric oxide: NO), プロスタグランジン (PGI₂) などがある。川崎病の急性期にはeNOS (endothelial nitric oxide synthase) およびiNOS (inducible nitric oxide synthase) の両方の発現が亢進しているが、主たるものはiNOS発現の亢進である。川崎病の初期における単球/マクロファージを中心とした炎症性サイトカインの作用により、iNOSを介した大量のNOが産生され、これが活性酸素と結合してパーオキシナイトライトを産生し、組織障害を惹起し、血管炎、血栓症を増悪し、新生内膜増殖を促進する¹⁵⁾。iNOSのプロモーター領域にはNF- κ B結合部位が同定されており、その活性が他の転写因子とともにiNOS発現に重要な役割を果たしている。

一方、PGI₂は血管平滑筋拡張作用、血小板凝集抑制作用などを有し、主に血小板から産生され、血管収縮作用、血小板凝集作用を有するTXA₂ (thromboxane A₂) に相反する。川崎病の初期には、TXA₂の増加が著明で、TXA₂/PGI₂比は有意に高値を呈し、血管収縮作用、血小板凝集作用の亢進がうかがわれる。しかし、 γ グロブリン療法後にはTXA₂は有意に低下し、TXA₂/PGI₂比は改善し、血管壁における血管収縮・血小板凝集反応は恒常性が保たれる¹⁶⁾。

b) 血管収縮・血小板凝集・細胞増殖作用因子

血管内皮細胞で産生されるET-1 (endothelin-1) は血管平滑筋細胞に発現しているET-A受容体を介して、強力で持続的な血管収縮作用、血管平滑筋増殖作用を、また、血管内皮細胞に発現しているET-B受容体を介して、NOやプロスタサイクリンなどの血管拡張因子の遊離に関与する。川崎病の急性期にはET-1は有意に上昇する。特に、冠動脈障害を合併した症例での血漿中の濃度は冠動脈障害を合併していない症例に比し、有意に高く、冠動脈障害発生の予知因子となり得る¹⁷⁾。

c) 細胞増殖因子

川崎病の急性期において、血管新生や血管内皮細胞に対する増殖作用、遊走作用、血管透過性亢進作用などを有するVEGF (vascular-endothelial growth factor) は有意に増加し¹⁸⁾、更にその受容体の発現も亢進し、低アルブミン血症や血管拡張の一因となる¹⁹⁾。一方、遠隔期の虚血心筋においては血管新生を促す作用を有する。また、VEGFは血管内皮細胞や血管平滑筋細胞に作用して、細胞外基質を破壊し、瘤形成を助長させるMMPs (matrix metalloproteinases) の産生に関与する。川崎病の初期には血漿中のMMP-1, -2, -3, -9が有意に増加し、 γ グロブリン療法により低下する。更に、MMPの抑制因子であるTIMP-1 (tissue inhibitor of metalloproteinase), TIMP-2も病初期に増加する。MMPとMMP/TIMPの不均衡が冠動脈病変の形成にかかわっている可能性が指摘されている²⁰⁾。

表 1 川崎病の各種病態におけるバイオマーカー

各種病態	バイオマーカー
血管炎・血管障害	hs-CRP(high-sensitive C-reactive protein), SAA(serum amyloid-A), PTX3(pentraxin3), ET-1(endothelin-1), CNP(C-type natriuretic peptide), など
心室収縮・弛緩能の異常	BNP(brain natriuretic peptide), NT-proBNP(N-terminal pro-brain natriuretic peptide), など
心筋障害(壊死)	筋原線維マーカー: TnT(troponinT), TnI(troponinI), など 細胞質マーカー: H-FABP(heart-type fatty acid binding protein), など
凝固線溶系	TF(tissue factor), PAI-1(plasminogen activator inhibitor-1), など

更に、川崎病の急性期には細胞の分化や増殖を調節する多機能分泌蛋白である TGF- β (transforming growth factor- β) が増加する¹⁹⁾。細胞外マトリックスの分解に関与するプロテアーゼである MMP の抑制因子である TIMP-1 の発現を誘導し、平滑筋細胞の遊走、増殖を抑制する。更に、心筋虚血部位の血管新生にも関与する。

c. 冠動脈障害、心筋障害と各種バイオマーカーの変動(表 1)

川崎病の主たる病態は血管炎であり、その血管炎のマーカーとしては hs-CRP(high-sensitive C-reactive protein) や serum amyloid-A(SAA)²¹⁾, pentraxin3(PTX3)²²⁾ などが最近注目されている。PTX3 は炎症に伴いサイトカインによりマクロファージ、血管内皮細胞などから分泌される。冠動脈障害をみるうえでのバイオマーカーとしては血管内皮細胞より産生される ET-1, C 型ナトリウム利尿ホルモン(CNP) が有用と思われる。ただし、現在 CNP の測定はコマーシャルベースにては実現していない。

一方、川崎病ではその初期に軽度で可逆的な心筋炎を合併することがあるとされている。川崎病の病初期に心室筋のストレスマーカーである、BNP(brain natriuretic peptide) が有意に増加し、心室収縮・弛緩能の異常をよく反映しているとの報告が散見される^{23,24)}。病初期の心筋炎や回復期以降に認められる心筋虚血に伴う心筋障害の評価の一指標に BNP はなり得ると思われる。更に、急性心筋梗塞時の心筋障害(壊

死)マーカーとしては、心筋トロポニン T(TnT)、心筋トロポニン I(TnI)、および心筋型脂肪酸結合蛋白(H-FABP)が有用である。特に H-FABP は急性心筋梗塞発症より 1-2 時間後より上昇するので、早期診断に有用である。一方、トロポニンは発症 3-4 時間後から上昇し、異常値が長期間(TnT: 8-12 日, TnI: 5-8 日)持続するので、その後の診断に有用である。我が国では TnT および H-FABP の定性測定キットである トロップ T センシティブ、ラピチェック H-FABP が市販されている。また、凝固・線溶系のマーカーとしては TF(tissue factor), PAI-1(plasminogen activator inhibitor-1) が有用である。更に、遠隔期における動脈硬化を含む冠動脈障害の病態を炎症マーカーである hs-CRP, SAA がよく反映しているとの報告もある²⁵⁾。今後川崎病の各病態の評価にバイオマーカーが汎用される時代の到来が望まれる。

おわりに

川崎病に特徴的な血液検査所見はなく、血液検査だけで鑑別診断をすることは不可能である。ただし、幾つかの検査所見をピックアップし、経時的に follow up することにより、川崎病の各種病態の把握、治療戦略の構築および治療効果の評価、予後判定などが可能となる。今後、新たな血液関連因子の発見、検査法の開発などにより、更なる川崎病の診断、治療への貢献が期待される。

文 献

- 1) Shikishima Y, et al: Inverse correlation between macrophage-colony stimulating factor, cholesterol and high density lipoprotein cholesterol in Kawasaki disease. *Asian Pac Allergy Immunol* 19: 85-91, 2001.
- 2) Cheung YF, et al: Induction of MCP-1, CCR2, and iNOS expression in THP-1 macrophages by serum of children late after Kawasaki disease. *Pediatr Res* 58: 1306-1310, 2005.
- 3) Melish ME, Hicks RV: Kawasaki syndrome: clinical features. Pathophysiology, etiology and therapy. *J Rheumatol Suppl* 24: 2-10, 1990.
- 4) Koike R: The effect of immunoglobulin on immune complexes in patients with Kawasaki disease (MCLS). *Acta Paediatr Jpn* 33: 300-309, 1991.
- 5) Lin CY, et al: Serial changes of serum interleukin-6, interleukin-8, and tumor necrosis factor alpha among patients with Kawasaki disease. *J Pediatr* 121: 924-926, 1992.
- 6) Furukawa S, et al: Kawasaki disease differ from anaphylactoid purpura and measles with regard to tumor necrosis factor-alpha and interleukin 6 in serum. *Eur J Pediatr* 151: 44-47, 1992.
- 7) Suzuki H, et al: Effects of immunoglobulin and gamma-interferon on the production of tumor necrosis factor-alpha and interleukin-1 beta by peripheral blood monocytes in the acute phase of Kawasaki disease. *Eur J Pediatr* 155: 291-296, 1996.
- 8) Asano T, Ogawa S: Expression of monocyte chemoattractant protein-1 in Kawasaki disease: the anti-inflammatory effect of gamma globulin therapy. *Scand J Immunol* 51: 98-103, 2000.
- 9) Asano T, Ogawa S: Expression of IL-8 in Kawasaki disease. *Clin Exp Immunol* 122: 514-519, 2000.
- 10) Jibiki T, et al: High concentrations of interleukin-8 and monocyte chemoattractant protein-1 in urine of patients with acute Kawasaki disease. *Eur J Pediatr* 163: 749-750, 2004.
- 11) Inoue Y, et al: Increased circulating granulocyte colony-stimulating factor in acute Kawasaki disease. *Pediatr Int* 41: 330-333, 1999.
- 12) Oana S, et al: Serum M-CSF levels in Kawasaki disease. *Br J Haematol* 107: 462-463, 1999.
- 13) Furukawa S, et al: Increased levels of circulating intercellular adhesion molecule 1 in Kawasaki disease. *Arthritis Rheum* 35: 672-677, 1992.
- 14) Kim DS, Lee KY: Serum soluble E-selectin levels in Kawasaki disease. *Scand J Rheumatol* 23: 283-286, 1994.
- 15) Iizuka T, et al: Nitric Oxide and aneurysm formation in Kawasaki disease. *Acta Paediatr* 86: 470-473, 1997.
- 16) 鶴田恵子: 川崎病急性期におけるガンマグロブリン投与前後の尿中トロンボキサンA2とプロスタサイクリン代謝産物の検討. *日児誌* 100: 1729-1734, 1996.
- 17) Ogawa S, et al: Increased plasma endothelin-1 concentration in Kawasaki disease. *J Cardiovasc Pharmacol* 22: S364-S366, 1993.
- 18) Maeno N, et al: Increased serum levels of vascular endothelial growth factor in Kawasaki disease. *Pediatr Res* 44: 596-599, 1998.
- 19) Yasukawa K, et al: Systemic production of vascular endothelial growth factor and fms-like tyrosine kinase-1 receptor in acute Kawasaki disease. *Circulation* 105: 766-769, 2002.
- 20) Senzaki H: The pathophysiology of coronary artery aneurysms in Kawasaki disease: role of matrix metalloproteinases. *Arch Dis Child* 91: 847-851, 2006.
- 21) Blake GJ, Ridker PM: Novel clinical markers of vascular wall inflammation. *Circ Res* 89: 763-771, 2001.
- 22) Mantovani A, et al: The long pentraxin PTX3 in vascular pathology. *Vascul Pharmacol* 45: 326-330, 2006.
- 23) Kurotobi S, et al: Brain natriuretic peptide as a hormonal marker of ventricular diastolic dysfunction in children with Kawasaki disease. *Pediatr Cardiol* 26: 425-430, 2005.
- 24) Takeuchi D, et al: Abnormal tissue Doppler images are associated with elevated plasma brain

- natriuretic peptide and increased oxidative stress in acute Kawasaki disease. *Circ J* 71: 357-362, 2007.
- 25) Mitani Y, et al: Elevated levels of high-sensitive C-reactive protein and serum amyloid-A later after Kawasaki disease: association between inflammation and late coronary sequelae in Kawasaki disease. *Circulation* 111: 38-43, 2005.

Coronary Artery Aneurysm Induced by Kawasaki Disease in Children Show Features Typical Senescence

Ryuji Fukazawa, MD; Ei Ikegami, MD; Miki Watanabe, MD; Miharuru Hajikano, MD; Mitsuhiro Kamisago, MD; Yasuhiro Katsube, MD; Hitoshi Yamauchi, MD*; Masami Ochi, MD*; Shunichi Ogawa, MD

Background Kawasaki disease (KD) causes coronary artery disease (CAD) in children. In addition, a history of KD is suspected to be a risk factor for the development of atherosclerotic heart disease in the future. Histological senescence changes are a common denominator in atherosclerotic lesions in adults, so the present study investigated whether histological senescence changes had already occurred in KD aneurysm.

Methods and Results KD coronary aneurysms and internal mammary arteries retrieved from 5 children with KD (3, 4, 5, 6, and 11 years old, respectively) who underwent coronary artery bypass grafting, as well as giant coronary aneurysm size-reducing operations, were analyzed. Senescence-associated strong β -galactosidase activity was observed in KD aneurysms, but not in the internal mammary arteries. An immunohistochemical analysis of the KD aneurysm using anti-CD31, anti-endothelial nitric oxide synthetase (eNOS), anti-vascular adhesion molecule-1 (VCAM-1), and anti-monocyte chemoattractant protein-1 (MCP-1) showed vascular endothelium CD31 staining, decreased staining of eNOS and strong staining of MCP-1 and VCAM-1. cDNA microarray gene expression profiling revealed increased MCP-1 expression in the KD aneurysm, a finding confirmed by quantitative polymerase chain reaction.

Conclusions Histological features of senescence and active remodeling gene expression show that the KD aneurysm is not a silent vasculitis terminal. The future fate of KD aneurysms, including atherosclerosis, should be monitored carefully. (*Circ J* 2007; 71: 709–715)

Key Words: Aneurysm; Atherosclerosis; Kawasaki disease; Senescence

Kawasaki disease (KD) is known to cause coronary artery disease (CAD) in approximately 10,000 children in Japan every year,¹ and preventing this outcome is the ultimate goal of treating the acute phase of KD. In addition to being a cause of acute phase CAD, it has recently been suggested that a history of KD may itself be one of the risks for future atherosclerosis.^{2,3} Mitani et al⁴ showed elevated levels of high-sensitivity C-reactive protein in KD patients with a coronary artery aneurysm, which suggests a risk for developing atherosclerosis and other vascular maladies in late phase KD.

Recent findings suggest that atherosclerosis is an inflammatory disorder^{5, 7} and that vascular senescence plays an essential role in its development.^{8,9} Vascular senescence findings include increased adhesion molecules and pro-inflammatory cytokines or chemokines, as well as a reduction of normal physiological vascular proteins, such as endothelial nitric oxide synthetase (eNOS) and prostacyclins. All of these histological vascular senescence features are observed around atherosclerotic plaques.¹⁰

A recent report by Suzuki et al suggests there are histological differences between KD coronary artery and adult atherosclerotic plaque.¹¹ There is a different distribution of the expression of growth factors between the KD and athero-

sclerosis lesions, but we assume that smooth muscle cell growth and vascular remodeling, as the response to growth factors and inflammatory cytokines, is the basic biological response to vascular tissue inflammation. As long as KD vasculitis and atherosclerosis are based on an inflammatory reaction, there should be pathophysiological and genetic similarities as well as differences. We suspect that similar inflammatory reactions may facilitate the post-KD coronary artery in making atherosclerotic lesions. We hypothesize that vascular senescence has already appeared in the KD-affected vasculature and might contribute to future atherosclerosis. Typical vascular senescence findings are increase of β -galactosidase (β -gal) activity, as well as a decrease of the vascular physiological protein eNOS.⁹ In addition, increased adhesive proteins, such as vascular adhesion molecule-1 (VCAM-1)⁶ as well as increased chemokines, such as chemokine monocyte chemoattractant protein-1 (MCP-1)^{12,13} are major vascular histological findings in the atherosclerosis lesion. In the present study we examined whether these histological characteristics might have already appeared in the KD aneurysm, and whether gene expression profiling by cDNA microarray might show what is proceeding in KD aneurysm. This study is the first to analyze the KD aneurysm from the standpoint of vascular senescence.

Methods

Chemicals

All chemicals were purchased from Sigma-Aldrich (St Louis, MO, USA) unless noted otherwise.

(Received August 17, 2006; revised manuscript received February 13, 2007; accepted February 21, 2007)

Department of Pediatrics and *Department of Surgery, Cardiovascular Surgery, Nippon Medical School, Tokyo, Japan
Mailing address: Ryuji Fukazawa, MD, Department of Pediatrics, Nippon Medical School Tama-Nagayama Hospital, 1-7-1 Tama, Tokyo 206-8512, Japan. E-mail: oraora@nms.ac.jp

Table 1 Patients' Backgrounds

Case no.	Gender	Age at onset	Age at CABG	Aneurysm site size (mm)	Stenosis	Acute phase therapy	Maintenance therapy	Operative procedure
1	M	4y3m	5y3m	LAD: 38.9, RCA: 35.0	(-)	IVIG, Steroid pulse, Ulinastatin	Warf, Asp, Dipy	LITA-LAD, RCA plication
2	M	1y1m	3y1m	LAD: 19.8	(-)	IVIG	Asp, Ticlopidine	LITA-LAD, LCA plication
3	M	8y7m	11y4m	LAD: 16.0, RCA: 17.0	#7	IVIG, Ulinastatin	Warf, Asp, Carteolol	LITA-LAD, RCA plication
4	F	1y1m	11y2m	LAD: 30.7, RCA: 18.8	(-)	IVIG, Steroid	Warf, Asp, Dipy, Propranolol	LITA-LAD-D1-Cx, RCA plication
5	M	3y6m	6y1m	LAD: 33.6, RCA: 76.3	(-)	IVIG, Ulinastatin	Warf, Heparin div	LITA-LAD, RCA plication

CABG, coronary artery bypass grafting; y, year; m, month; LAD, left anterior descending coronary artery; RCA, right coronary artery; IVIG, intravenous immunoglobulin therapy; Steroid pulse, steroid pulse therapy; Warf, warfarin; Asp, aspirin; Dipy, dipyridamole; LITA, left internal thoracic artery; LCA, left coronary artery; D1, first diagonal branch; Cx, circumflex artery; div, dripping intravenous infusion.

Table 2 Differences in the Gene Expression of the KD Aneurysm Tissue and ITA

Ratio	Difference	Gene bank code	Gene
0.45	-19,662	M36711	Transcription factor AP-2 (TFAP2: AP2TF)
0.64	-19,379	M26880	Ubiquitin
Undefined	-18,755	M97796	Helix-loop-helix protein; DNA-binding protein inhibitor Id-2
0.46	-18,426	M83221	I-rel (RELB)
0.55	-18,012	X69391	60S ribosomal protein L6 (RPL6)
0.32	-17,375	M73780	Integrin β 8 precursor (ITGB8)
0.52	-16,631	X06820	Transforming protein rhoB; ARHB; ARH6
0.49	-16,107	M63896	Transcriptional enhancer factor (TEF1)
0.41	-15,573	U10550	Ras family member (ras-like protein KIR)
0.32	-14,178	X93499	Ras-related protein RAB-7
0.21	-14,087	X51405	Carboxypeptidase H precursor (CPH)
0.37	-13,443	U78576	68-kDa type I phosphatidylinositol-4-phosphate 5-kinase α
0.34	-11,428	AJ000512	Stimulus- & glucocorticoid-regulated serine/threonine protein kinase (SGK)
0.42	-11,349	X07270	Heat shock 90-kDa protein A (HSP90A)
0.52	-11,226	U48959	Myosin light chain kinase (MLCK) smooth muscle & non-muscle isozymes
4.41	10,313	SS6143	Adenosine A1 receptor (ADORA1)
Undefined	10,376	M62424	Thrombin receptor (TR)
Undefined	10,381	X04429	Endothelial plasminogen activator inhibitor-1 precursor (PAI1)
5.16	10,664	L12350	Thrombospondin 2 precursor (THBS2)
2.09	10,957	X04106	Calpain; calcium-activated neutral proteinase (CANP)
11.80	12,228	X66365	Cell division protein kinase 6 (CDK6)
7.89	12,807	X69550	Rho GDP dissociation inhibitor 1 (RHO-GDI 1)
Undefined	13,101	AF013263	Apoptotic protease activating factor 1 (APAF1)
4.50	15,270	V00568	C-myc oncogene
23.34	15,663	X57766	Matrix metalloproteinase 11 (MMP11)
16.75	17,217	U51004	Hint protein; protein kinase C inhibitor 1 (PKC11)
Undefined	20,178	M68867	Cellular retinoic acid-binding protein II (CRABP2)
39.73	22,386	M12529	Apolipoprotein E precursor (APOE)
1.96	26,570	M24545	Monocyte chemoattractant protein 1 precursor (MCP1)
Undefined	29,200	X03124	Metalloproteinase inhibitor 1 precursor (TIMP1)
2.80	35,111	M92381	Thymosin β -10 (TMSB10)
5.44	37,928	X05562	Procollagen α 2 (IV) subunit precursor

KD, Kawasaki disease; ITA, intrathoracic artery.

The signals of 5 membranes each of ITA tissue and KD aneurysm were averaged.

Averaged Array 1 (A1) was ITA tissue and averaged Array 2 (A2) was KD aneurysm tissue.

Ratio: ratio of the signal from A2 compared with A1.

Ratio = A2 intensity/A1 intensity, Undefined: gene signal α ; background level in 1 array.

Difference: The signal difference of A2 compared with A1

Difference = A2 intensity - A1 intensity.

When the ratio was over 1.5 (or below 0.67), and the difference was over/under 1,000, gene expression difference was considered prevalent and was listed on the Table.

Preparation of Coronary Artery Tissues

Five patients (age: 7.4 ± 1.7 years) with KD who had giant coronary aneurysms underwent coronary artery bypass grafting (CABG) because of myocardial ischemia induced by coronary artery stenosis. The mean time from KD onset to CABG was 3.7 ± 1.6 years. These patients also had aneurysm size-reduction procedures (plication) as an adjunct

operation (Table 1) and so our specimens were from the center of the giant aneurysms. We conducted this procedure when the patients underwent CABG, in addition, thrombus formation was uncontrollable, even with warfarin anticoagulation therapy, because of the size of the aneurysms.^{1,4} Shear stress to the vascular wall is inversely proportional to vascular radius, so an increase in shear stress was expected

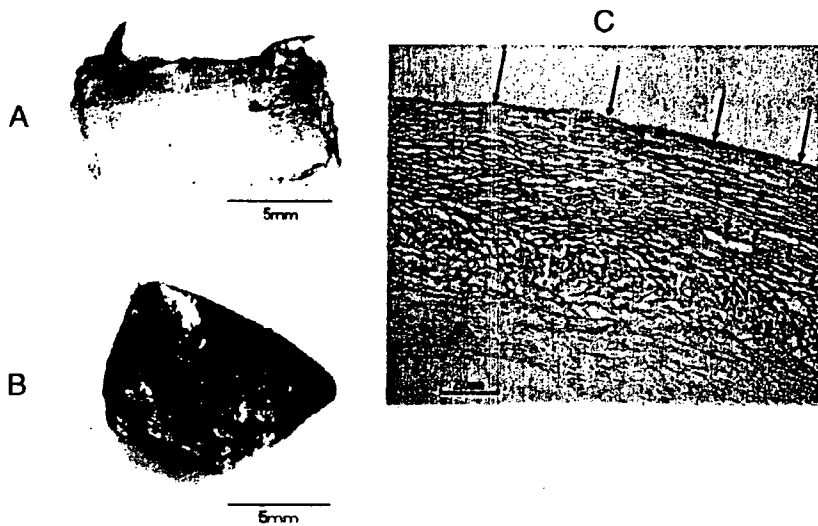


Fig 1. Senescence-associated β -galactosidase (β -gal) staining. (A) Control ITA: slight β -gal activity (blue staining) can be seen on the luminal surface. (B) Giant coronary artery aneurysm of a KD patient: strong senescence associated β -gal activity (blue staining) can be seen on the luminal surface of the aneurysm. (C) Frozen cross-section of β -gal-stained KD aneurysm: the blue color is mainly localized inside the aneurysm, suggesting that β -gal activity is mainly by endothelial cells (long arrows). Beta-gal activity is also observed on the adventitial side of the KD aneurysm (short arrows), suggesting senescence changes are also occurring at this location. KD, Kawasaki disease; ITA, internal thoracic artery.

with reduction of the radius of the aneurysm. It was also anticipated that turbulent flow in the aneurysm would become pulsatile and that coronary flow velocity would be increased.⁵ Reducing the vascular radius and increasing the flow velocity both contribute to augmentation of vascular shear stress and this protects against thrombus formation in the aneurysm.⁶ Therefore, we expected that the plication procedure would greatly assist the anticoagulation therapy. The excised coronary arteries were the subject of our analysis and the internal thoracic arteries (ITA), trimmed for CABG, were used as controls. This study was approved by the Nippon Medical School Ethics Committee and written informed consent was given by the patients' parents.

Senescence-Associated β -Gal Activity

Senescence-associated β -gal activity was examined in the tissues as described previously.⁹ Briefly, the samples were fixed in 4% paraformaldehyde (PFA) for 30 min at room temperature and incubated for 24 h at 37°C in freshly prepared β -gal staining solution containing 1 mg/ml 5-bromo-4-chloro-3-indolyl β -D-galactopyranoside (X-gal), 5 mmol/L potassium ferrocyanide, 5 mmol/L potassium ferricyanide, 150 mmol/L NaCl, 2 mmol/L MgCl₂, 0.01% sodium deoxycholate, and 0.02% Nonidet-40. After the stained arteries were photographed, the samples were immersed in OCT compound (Sakura Finetechnical Co Ltd, Tokyo, Japan) and frozen in dry ice prior to cryostat sectioning.

cDNA Microarray Gene Expression Profiling

Excised arterial tissue was immersed immediately in RNAlater stabilization reagent (QIAGEN Science, MD, USA), and the RNA was extracted using the RNeasy mini kit (QIAGEN Science). Contaminating DNA was removed using an RNase-free DNase kit (QIAGEN Science). Total RNA was treated as the starting material for cDNA microarray analysis (Human ATLAS 1.2, BD Bioscience Clontech, Palo Alto, CA, USA) following the manufacturer's protocol. Briefly, a probe was synthesized from over 3 μ g of the total RNA and dATP-P³², and was hybridized overnight at 68°C to the micro-array membranes. Thereafter, the membranes were washed several times and exposed to X-ray film for up to 1 week. The X-ray films were scanned (ES-2000 EPSON) and the data were analyzed using ATLAS Image 1.5 software (BD Bioscience Clontech). The gene

expression signal of each of the 5 membranes per tissue sample (5 ITA samples, 5 coronary artery aneurysm samples) was averaged by the software, and compared. We defined Array1 as the ITA, and Array2 was as the aneurysm. The ratio and difference in the signals were calculated as follows: ratio=(signal intensity from Array2 (A2))/(signal intensity from Array1 (A1)), difference=(A2)-(A1). When the ratio was over 1.5 (or below 0.67), and the difference was over/under 1,000, gene expression difference was considered prevalent (Table 2).

Quantitative Polymerase Chain Reaction (PCR) for MCP-1 Expression

The primers and probe for MCP-1 were designed according to the cDNA sequence (Gene Bank S69738) using Primer Express software (Applied Biosystems, Foster City, CA, USA). Forward primer: 5'CGCCTCCAGCATGAAA-GTCT3'; reverse primer: 5'GGGAATGAAGGTGGCTG-CTA3', and Probe 5'-(6-Fam)-CGCCCTTCTGTGCCTG-CTGCT-(Tamra) (Phosphate)-3'. The β -actin primers and probe were purchased from Applied Biosystems. The RNA obtained from the aneurysm and ITA was reverse transcribed using a reverse transcription PCR (RT-PCR) kit (Takara Bio Inc, Ohtsu, Japan). Quantitative PCR for MCP-1 was performed with the GeneAmp 5700 Sequence Detection System (Applied Biosystems). The amounts of β -actin were simultaneously measured and the ratio of MCP-1 to β -actin was calculated. The data are expressed as mean \pm SE. MCP-1 expression was compared between the aneurysm and ITA samples by Student's t-test using StatView 5.0 (SAS Institute Inc Cary, NC, USA).

Immunohistochemistry

The excised tissue samples were fixed in 4% PFA, embedded in paraffin, and sliced into 4- μ m sections. Following de-paraffinization and heat antigen retrieval, the primary antibodies were loaded after intrinsic peroxidase blocking. Working dilutions of the primary antibodies were as follows: anti-CD31 (1:50, clone JC70A, Dako Cytomation, Location, Glostrup, Denmark), anti-eNOS (1:75, clone 3, BD Biosciences Pharmingen, San Jose, CA, USA), anti-VCAM-1 (1:50, H-276, Santa Cruz Biotechnology Inc Santa Cruz, CA, USA) and anti-MCP-1 (1:10, ab7814, Abcam, Cambridge, UK). Antibody signals were detected by a

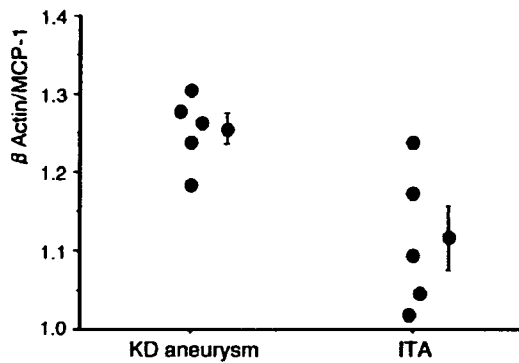


Fig 2. Quantitative PCR shows increased MCP-1 expression in the KD aneurysm and that the ratio of MCP-1 expression to β -actin expression is significantly higher in the KD aneurysm samples than in the ITA samples. The β -actin/MCP-1 was 1.25 ± 0.05 in the aneurysm and 1.11 ± 0.09 in the ITA ($p=0.015$). KD, Kawasaki disease; ITA, internal thoracic artery; PCR, polymerase chain reaction; MCP-1, monocyte chemoattractant protein-1.

Dako envision/HRP kit. Peroxidase activity was visualized by 0.02% 3-3' diaminobenzidine and 0.05% hydrogen peroxide (Dako Cytomation).

Results

Senescence-Associated β -Gal Activity Staining

Beta-gal activity was hardly detected in the ITA samples (Fig 1A), but in the aneurysm samples there was strong activity on both the intimal surface (Fig 1B), corresponding to the vascular endothelium, and on the adventitia (Fig 1C).

cDNA Microarray Gene Expression Profiling

The gene expression differences between the aneurysm and ITA samples are shown in Table 2. The genes that were significantly expressed in the aneurysm samples were pro-collagen $\alpha 2$ (IV) subunit precursor, metalloproteinase inhibitor 1 precursor (TIMP1), MCP-1, matrix metalloproteinase 11 (MMP11), and apoptotic protease activating factor 1 (APAF1).

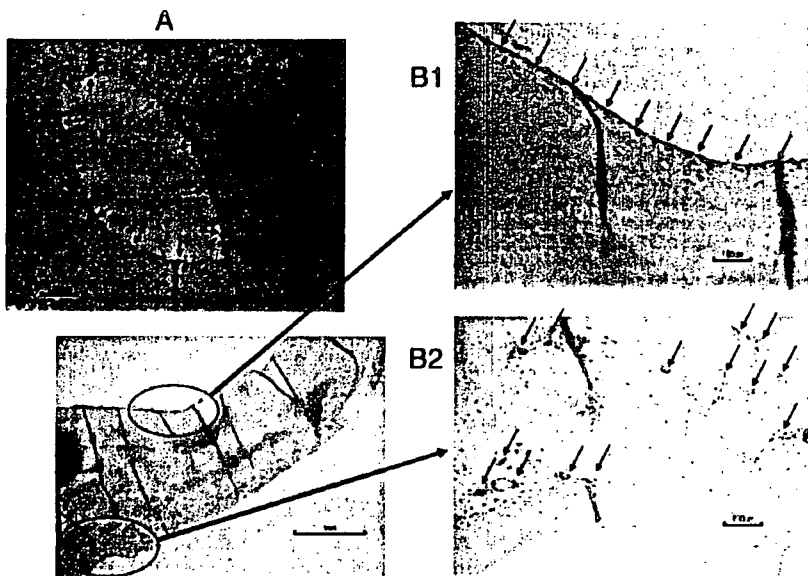


Fig 3. Immunohistochemical staining for CD31. (A) Control ITA: positive staining can be seen along the intimal endothelium (arrows). (B) KD aneurysm: intimal endothelium (B1, arrows), as well as the endothelium of the vasa vasorum, is positive (B2, arrows). KD, Kawasaki disease; ITA, internal thoracic artery.

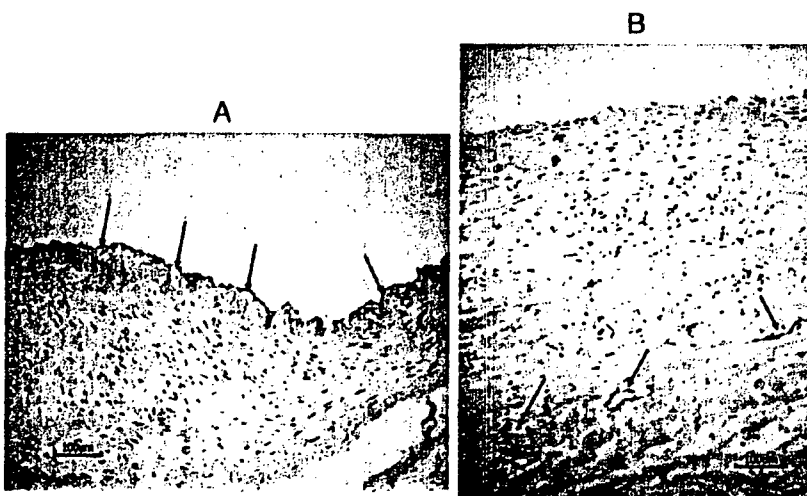


Fig 4. Immunohistochemical staining for eNOS. (A) Control ITA: positive stained along the endothelium (arrows). (B) KD aneurysm: negative staining of the intimal endothelium, but positive along the endothelium of the vasa vasorum (arrows). eNOS, endothelial nitric oxide synthetase; KD, Kawasaki disease; ITA, internal thoracic artery.

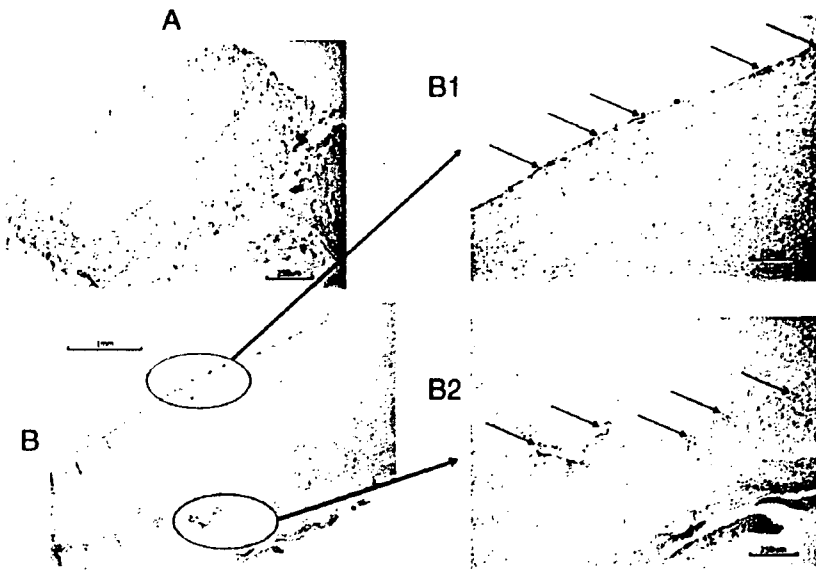


Fig 5. Immunohistochemical staining for VCAM-1. (A) Control IMA: negative staining. (B) KD aneurysm: VCAM-1 staining mainly in the vasa vasorum (B2, arrows) and the intimal endothelium (B1, arrows). KD, Kawasaki disease; VCAM-1, vascular adhesion molecule-1. IMA, internal mammary artery.

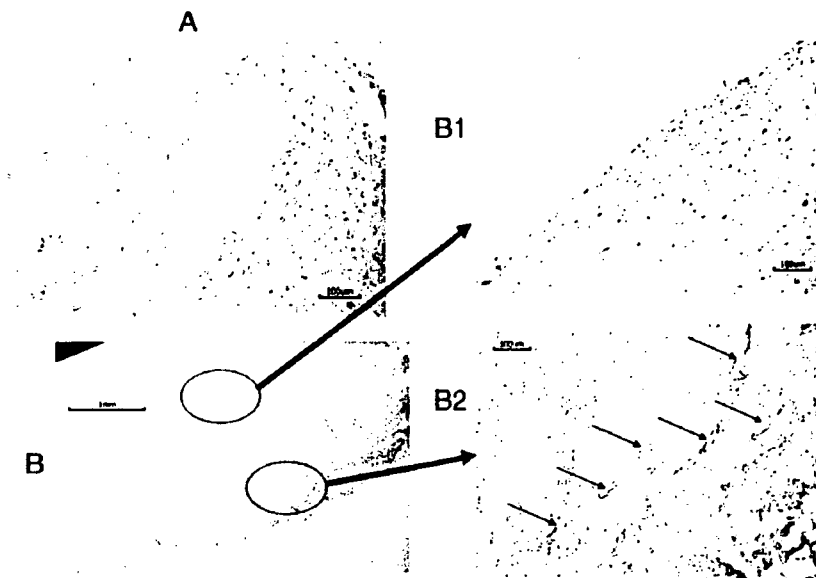


Fig 6. Immunohistochemical staining for MCP-1. (A) Control IMA: negative staining. (B) KD aneurysm: MCP-1 staining in the vasa vasorum (B2, arrows), but not on the intimal endothelium (B1). KD, Kawasaki disease; MCP-1, monocyte chemoattractant protein-1; IMA, internal mammary artery.

MCP-1 Quantitative PCR

MCP-1 expression was significantly increased in the aneurysm samples compared with the IMA samples (Fig 2). The β -actin/MCP-1 ratio was 1.25 ± 0.05 for aneurysm tissue and 1.11 ± 0.09 for IMA tissue, which was a significant difference ($p=0.015$).

Immunohistochemistry

CD31 was stained in the endothelium of both IMA and aneurysm samples (Figs 3A,B). In addition, CD31 was present in the vasa vasorum of the aneurysm (Fig 3B2).

In the control IMA, eNOS was detected along the vascular endothelium (Fig 4A), but was hardly detected on the endothelial surface of the aneurysm samples (Fig 4B). In contrast, eNOS was highly expressed in the vasa vasorum in the aneurysms (Fig 4B).

None to minuscule VCAM-1 staining was observed in the IMA (Fig 5A), but the endothelium of the intimal surface of the aneurysm (Fig 5B1), and of the vasa vasorum,

was well stained with VCAM-1 (Fig 5B2).

None to minuscule MCP-1 staining was observed in the IMA (Fig 6A), but was detected in the vasa vasorum of the aneurysms (Fig 6B2), although not in the intimal endothelium (Fig 6B1).

Discussion

The histological features of KD coronary lesions are destruction of the 3 layers of vessel walls and significant intimal hyperplasia,⁷ and to date KD has been considered as a specific vasculitis of children only. Recent immunohistological studies suggest that KD coronary artery lesions are not silent terminal tissue after vasculitis. They actively produce inflammatory cytokines¹⁸ and were still in the active remodeling state!¹¹ In the present study we also confirmed high expression of genes associated with vascular remodeling, such as procollagen $\alpha 2$, TIMP1, MCP-1, MMP11, and APAF1, in the KD aneurysm, suggesting active remodeling

was taking place. Furthermore, we detected increased senescence-associated β -gal activity in the adventitia and the luminal surface of the endothelium. Both MCP-1 and VCAM-1 were strongly expressed in the vasa vasorum of the adventitia. Miura et al¹⁹ also reported expression of cell adhesion molecules, including VCAM-1, in the neovascularization of KD coronary arteries. All of these findings suggest that the KD aneurysm is not terminal silent debris after severe vasculitis. High expression of extracellular matrix, such as procollagen α , may facilitate vascular stiffness or vascular sclerosis. Intriguingly, VCAM-1 and MCP-1 were mainly expressed in the vasa vasorum of the KD aneurysm, which we consider is a histological finding that is unique to KD and different from that of adult atherosclerosis lesions, and that it suggests a distinct disease progression. Although adult atherosclerosis progression originates from the intimal side of the arteries, the sclerotic change of the KD aneurysm may develop from the adventitial vasa vasorum. We propose that vascular disease progression in KD differs from that of adult atherosclerosis.

Not only are there differences, but there are also similarities between adult atherosclerosis and the KD aneurysm. One of the characteristic histological features in atherosclerosis is "vascular senescence", which includes a decrease in vasodilative factors, such as nitric oxide, and an increase in vascular wall stiffness, cell adhesion molecules, and inflammatory cytokines.¹⁰ Vascular senescence is closely related to atherosclerosis.¹⁰ This study is the first to demonstrate that vascular senescence is developing in the KD aneurysm. The intimal surface of the KD aneurysmal endothelium is often denuded in acute phase KD vasculitis,⁹ but we found that endothelial cells, as detected by positive CD31 staining, had regrown on the intimal surface of the late-stage KD aneurysm. However, the intimal side of the endothelium showed a decreased expression level of physiological proteins such as eNOS and increased levels of adhesion molecules such as VCAM-1, the latter being closely related to atherosclerosis.⁶ These findings, typical of histological senescence, are surely a sign of disease progression in the KD aneurysm, and lead to the suspicion of early atherosclerosis developing in a KD aneurysm.

However, it is ridiculous to think that vascular senescence is a specific finding only for atherosclerosis. Because atherosclerosis is one of the vascular inflammatory diseases,⁷ it is natural to think that the inflammatory reaction itself facilitates vascular senescence. The pro-inflammatory factors, such as chemokines, cytokines, inflammatory cells, vascular blood flow, and shear stress, are all important background mechanisms for vascular senescence. Therefore, we think it is no wonder that the KD aneurysm showed vascular senescence.

In this study, we examined the gene expression profiling of KD aneurysm tissue, and found a high expression of MCP-1, which was also confirmed by quantitative PCR. MCP-1 directs monocytes to the intima and plays a central role in the development of atherosclerotic plaques.²⁰ Several lines of evidence suggest that MCP-1 and its receptor CCR2 are involved in atherosclerosis.^{12,21} The MCP-1 gene polymorphism -2578G, which correlates with higher plasma levels of MCP-1, was associated with prevalent myocardial infarction in a large cohort.^{22,23} C-reactive protein is known to be a risk marker for vascular events,²⁴ and itself promotes MCP-1-mediated monocyte chemotaxis.²⁵ As well as adult atherosclerosis, MCP-1 also correlates with acute phase KD vasculitis.^{18, 26} Terai et al¹⁸ have reported profuse extra-

cellular matrix-bound MCP-1 expression on the adventitia and massive mononuclear cell infiltration in a patient who died 14 days after KD onset. In the present study we showed that MCP-1 is still actively involved in late-phase KD; however, little invasion of macrophages or inflammatory mononuclear cells was observed in the present KD aneurysm (data not shown). Lack of macrophage infiltration has been reported by others¹¹ and is considered a distinct feature of the KD coronary artery lesion compared with atherosclerosis. Therefore, the upregulated MCP-1 in the late-phase KD aneurysm that we observed in the present study is not vascular inflammation persisting from acute-phase KD. It may be one of the reactions of vascular senescence. We could not answer why high expression of both MCP-1 and VCAM-1 did not induce infiltration of macrophages or other inflammatory cells into the late-phase KD aneurysm. It may be the relatively short time from the onset of KD. At the very least, together with the finding of vascular senescence, the KD aneurysm is under active remodeling. We can not discard the possibility of early atherosclerosis progression at younger ages, as Takahashi et al reported.³ We should carefully monitor KD coronary lesions for development into early atherosclerosis or other complicated vascular disease.

On the other hand, physiologically impaired endothelial function in the brachial artery after KD was noted in patients without coronary artery lesions.^{2,27,28} Those patients had reduced brachial artery flow-mediated dilation (FMD). FMD is dependent on the ability of the endothelium to release nitric oxide.²⁹ However, another group³⁰ reported FMD reduction only in cases of KD with moderate to severe CAD, not in those with normal to mild CAD. The issue is still controversial. We used the KD patients' ITA as control tissue and we observed eNOS staining along the intimal endothelium of the ITA. We could not detect further findings of senescence in the ITA. Although KD causes systemic vasculitis, ITA might be affected less by inflammation than either the brachial artery or coronary artery. As the coronary artery is the site of the most severe inflammation in KD, the degree of vasculitis is not homogeneous. Second, what we stained was eNOS antigen. We did not measure eNOS activity itself and this may be reduced in the ITA of KD patients, even though eNOS expression is not impaired. It is conceivable that the ITA are also affected by KD vasculitis to some extent, but not so severe to cause vascular senescence.

For the first time, we report evidence of senescence progression in the KD aneurysm. These histological findings are almost the same as those found in early atherosclerosis in adults. However, there are also histological differences between the KD aneurysm and atherosclerosis. The KD aneurysm is not a terminal phase of vasculitis, but instead is undergoing active vascular remodeling. Vascular senescence of the KD coronary lesion is a risk for future complicated vascular disease, including atherosclerosis, so patients must be carefully followed.

Acknowledgments

The authors thank Mrs Katsuko Honjo for excellent technical assistance. This study was financially supported partially by the Japan Society for the Promotion of Science (Grant-in-Aid for science research (C) 14570781 and 16591060).

References

1. Yanagawa H, Nakamura Y, Yashiro M, Oki I, Hirata S, Zhang T, et

- al. Incidence survey of Kawasaki disease in 1997 and 1998 in Japan. *Pediatrics* 2001; **107**: E33.
2. Noto N, Okada T, Yamasuge M, Taniguchi K, Karasawa K, Ayusawa M, et al. Noninvasive assessment of the early progression of atherosclerosis in adolescents with Kawasaki disease and coronary artery lesions. *Pediatrics* 2001; **107**: 1095–1099.
 3. Takahashi K, Oharaseki T, Naoe S. Pathological study of postcoronary arteritis in adolescents and young adults: With reference to the relationship between sequelae of Kawasaki disease and atherosclerosis. *Pediatr Cardiol* 2001; **22**: 138–142.
 4. Mitani Y, Sawada H, Hayakawa H, Aoki K, Ohashi H, Matsumura M, et al. Elevated levels of high-sensitivity C-reactive protein and serum amyloid-A late after Kawasaki disease: Association between inflammation and late coronary sequelae in Kawasaki disease. *Circulation* 2005; **111**: 38–43.
 5. Ross R. The pathogenesis of atherosclerosis: A perspective for the 1990s. *Nature* 1993; **362**: 801–809.
 6. Blankenberg S, Barbaux S, Tiret L. Adhesion molecules and atherosclerosis. *Atherosclerosis* 2003; **170**: 191–203.
 7. Sata M. Molecular strategies to treat vascular diseases. *Circ J* 2002; **67**: 983–991.
 8. Matsushita H, Chang E, Glassford AJ, Cooke JP, Chiu CP, Tsao PS. eNOS activity is reduced in senescent human endothelial cells: Preservation by hTERT immortalization. *Circ Res* 2001; **89**: 793–798.
 9. Minamino T, Miyauchi H, Yoshida T, Ishida Y, Yoshida H, Komuro I. Endothelial cell senescence in human atherosclerosis: Role of telomere in endothelial dysfunction. *Circulation* 2002; **105**: 1541–1544.
 10. Minamino T, Miyauchi H, Yoshida T, Tateno K, Komuro I. The role of vascular cell senescence in atherosclerosis: Antisenescence as a novel therapeutic strategy for vascular aging. *Curr Vasc Pharmacol* 2004; **2**: 141–148.
 11. Suzuki A, Miyagawa-Tomita S, Komatsu K, Nishikawa T, Sakomura Y, Horie T, et al. Active remodeling of the coronary arterial lesions in the late phase of Kawasaki disease: Immunohistochemical study. *Circulation* 2000; **101**: 2935–2941.
 12. Ikeda U, Matsui K, Murakami Y, Shimada K. Monocyte chemoattractant protein-1 and coronary artery disease. *Clin Cardiol* 2002; **25**: 143–147.
 13. Bursill CA, Channon KM, Greaves DR. The role of chemokines in atherosclerosis: Recent evidence from experimental models and population genetics. *Curr Opin Lipidol* 2004; **15**: 145–149.
 14. Yamauchi H, Ochi M, Fujii M, Hinokiyama K, Ohmori H, Sasaki T, et al. Optimal time of surgical treatment for Kawasaki coronary artery disease. *J Nippon Med Sch* 2004; **71**: 279–286.
 15. Ogawa S, Ohkubo T, Fukazawa R, Kamisago M, Kuramochi Y, Uchikoba Y, et al. Estimation of myocardial hemodynamics before and after intervention in children with Kawasaki disease. *J Am Coll Cardiol* 2004; **43**: 653–661.
 16. Kuramochi Y, Ohkubo T, Takechi N, Fukumi D, Uchikoba Y, Ogawa S. Hemodynamic factors of thrombus formation in coronary aneurysms associated with Kawasaki disease. *Pediatr Int* 2000; **42**: 470–475.
 17. Amano S, Hazama F, Hamashima Y. Pathology of Kawasaki disease: I. Pathology and morphogenesis of the vascular changes. *Jpn Circ J* 1979; **43**: 633–643.
 18. Terai M, Jibiki T, Harada A, Terashima Y, Yasukawa K, Tateno S, et al. Dramatic decrease of circulating levels of monocyte chemoattractant protein-1 in Kawasaki disease after gamma globulin treatment. *J Leukoc Biol* 1999; **65**: 566–572.
 19. Miura M, Garcia FL, Crawford SE, Rowley AH. Cell adhesion molecule expression in coronary artery aneurysms in acute Kawasaki disease. *Pediatr Infect Dis J* 2004; **23**: 931–936.
 20. Libby P, Sukhova G, Lee RT, Galis ZS. Cytokines regulate vascular functions related to stability of the atherosclerotic plaque. *J Cardiovasc Pharmacol* 1995; **25**: S9–S12.
 21. Martinovic I, Abegunewardene N, Seul M, Vosseler M, Horstlick G, Buerke M, et al. Elevated monocyte chemoattractant protein-1 serum levels in patients at risk for coronary artery disease. *Circ J* 2005; **69**: 1484–1489.
 22. McDermott DH, Yang Q, Kathiresan S, Cupples LA, Massaro JM, Keane JF Jr, et al. CCL2 polymorphisms are associated with serum monocyte chemoattractant protein-1 levels and myocardial infarction in the Framingham Heart Study. *Circulation* 2005; **112**: 1113–1120.
 23. Iwai N, Kajimoto K, Kokubo Y, Okayama A, Miyazaki S, Nonogi H, et al. Assessment of genetic effects of polymorphisms in the MCP-1 gene on serum MCP-1 levels and myocardial infarction in Japanese. *Circ J* 2006; **70**: 805–809.
 24. De Servi S, Mariani M, Mariani G, Mazzone A. C-reactive protein increase in unstable coronary disease cause or effect? *J Am Coll Cardiol* 2005; **46**: 1496–1502.
 25. Han KH, Hong K-H, Park J-H, Ko J, Kang D-H, Choi K-J, et al. C-Reactive protein promotes monocyte chemoattractant protein-1-mediated chemotaxis through upregulating CC chemokine receptor 2 expression in human monocytes. *Circulation* 2004; **109**: 2566–2571.
 26. Asano T, Ogawa S. Expression of monocyte chemoattractant protein-1 in Kawasaki disease: The anti-inflammatory effect of gamma globulin therapy. *Scand J Immunol* 2000; **51**: 98–103.
 27. Deng Y, Li T, Xiang H, Chang Q, Li C. Impaired endothelial function in the brachial artery after Kawasaki disease and the effects of intravenous administration of vitamin C. *Pediatr Infect Dis J* 2003; **22**: 34–39.
 28. Dhillon R, Clarkson P, Donald AE, Powe AJ, Nash M, Novelli V, et al. Endothelial dysfunction late after Kawasaki disease. *Circulation* 1996; **94**: 2103–2106.
 29. Rubanyi GM, Romero JC, Vanhoutte PM. Flow-induced release of endothelium-derived relaxing factor. *Am J Physiol Heart Circ Physiol* 1986; **250**: H1145–H1149.
 30. Ikemoto Y, Ogino H, Teraguchi M, Kobayashi Y. Evaluation of pre-clinical atherosclerosis by flow-mediated dilatation of the brachial artery and carotid artery analysis in patients with a history of Kawasaki disease. *Pediatr Cardiol* 2005; **26**: 782–786.

Original Article

Reduced shear stress and disturbed flow may lead to coronary aneurysm and thrombus formations

TAKASHI OHKUBO, RYUJI FUKAZAWA, EI IKEGAMI AND SHUNICHI OGAWA

*Department of Pediatrics, Nippon Medical School Hospital, Tokyo, Japan***Abstract**

Background: With Kawasaki disease it is important to clarify the mechanisms of coronary artery aneurysm and thrombus to avoid acute myocardial infarction. The authors tested the hypothesis that shear stress is reduced at coronary branching sites and in coronary artery aneurysms, and that this reduction of shear stress can promote formation of coronary artery aneurysms and thrombus.

Methods: The subjects were 111 children with Kawasaki disease with left coronary artery aneurysms, classified into three groups: giant coronary artery aneurysm ($n = 28$, diameter of coronary artery >8 mm), aneurysm ($n = 44$, diameter of coronary artery $=8$ mm), and normal-appearing coronary ($n = 39$). Averaged peak flow velocity (APV), flow patterns and shear stress were measured and calculated at normal-appearing coronary vessels, left coronary artery branching sites and intra-coronary aneurysm using flow wire, and coronary angiography. Also, presence and appearance of thrombus were detected by intravascular ultrasonography.

Results: The authors found that 90.3% of the coronary artery aneurysms occurred at major left coronary branching sites. APV and shear stress were significantly decreased in giant coronary artery aneurysms (APV, 7.1 ± 2.1 cm/s; shear stress, 3.8 ± 2.1 dyne/cm²) and at the left coronary artery branching site (APV, 9.1 ± 1.2 ; shear stress, 1 ± 6.2 3.0). In total, 20 of 24 thrombi were detected only in giant aneurysm, and all patients exhibited disturbed flow pattern in their giant coronary artery aneurysms.

Conclusions: Reduced shear stress and disturbed flow pattern may lead to coronary artery aneurysm and thrombus formation.

Key words

coronary aneurysm, Doppler flow wire, Kawasaki disease, shear stress, thrombosis.

An important complication of Kawasaki disease, which involves diffuse and systemic vasculitis, is thrombosis in coronary artery aneurysms, which often occurs in giant coronary aneurysms and can cause acute myocardial infarction.^{1,2} Therefore, it is important to clarify the mechanisms of formation of coronary aneurysm and thrombus, which may involve biochemical and biomechanical factors. In our laboratory, we have focused on rheological changes in coronary arteries. We hypothesize that shear stress, which is related to blood flow velocity, is reduced at coronary branching sites and in coronary aneurysms with a history of Kawasaki disease, and that this reduction of shear stress can promote formation of coronary artery aneurysm and thrombus. It has been reported that, in adults, atherosclerosis initially occurs at coronary artery branching and bending sites, where shear stress is relatively

low, and low shear rates allow more time for lipoproteins to enter the intima, and for adhesion of white blood cells.^{3,4}

We propose that, in Kawasaki disease, there are two mechanisms of thrombus formation related to changes in shear stress in coronary artery due to stenotic lesions and dilated lesions of coronary artery. At the coronary stenotic lesions, increased shear stress can directly expose and/or activate GPIIb/IIIa receptors, the ligand of which is vWF, and cause platelets to aggregate and form thrombi.⁵ In contrast, in coronary artery aneurysm, shear stress can be reduced due to decreased coronary flow velocity and dilation of coronary artery, and this reduced shear stress leads to thrombus formation because of thrombogenicity caused by decreased endothelial function, leading to increased platelet aggregation and coagulation, and decreased fibrinolysis.

We designed this study to test four predictions: (i) that aneurysms often form at major left coronary artery branching sites; (ii) that low shear stress at coronary artery branching site correlates with coronary artery aneurysm; (iii) that lower shear stress inside aneurysms correlates with greater size of aneurysms; and (iv) that reduced shear stress strongly correlates

Correspondence: Shunichi Ogawa, MD, Department of Pediatrics, Nippon Medical School Hospital, 1-1-5 Sendagi, Bunkyo-ku, Tokyo 113-8603, Japan. Email: boston@nms.ac.jp

Received 11 April 2005; revised 22 September 2005; accepted 27 November 2005.

with thrombus formation. We determined the localization of aneurysms, calculated shear stress at the coronary artery branching site and in the coronary artery aneurysms, and evaluated thrombosis in the aneurysms.

Methods

Subjects

The subjects were 111 patients with Kawasaki disease, from 2 to 15 years of age, who had aneurysms in the left coronary artery but had no history of acute myocardial infarction or congestive heart failure. These patients had no significant stenosis in the proximal or distal portions of their aneurysms. A 2-D echocardiography was used to diagnose coronary artery abnormalities. Time from onset of Kawasaki disease to the examinations in this study ranged from 4 to 152 months. All patients had taken 5 mg/kg per day Aspirin and/or Warfarin (international ratio of prothrombin time, 1.5–2.0) as anticoagulant therapy.

Quantitative coronary angiography

A 5F left Judkins catheter was placed at the left coronary ostium. Quantitative biplanes coronary angiography (CAG) was performed in all patients in 30° right anterior oblique view with 60° left anterior oblique view, and 60° right anterior oblique view with 30° left anterior oblique view. If other views were needed, some degree of caudal and/or cranial view with left and/or right oblique view was added. The percent stenosis, reference diameter of the adjacent normal-appearing segment, and minimal luminal diameter were calculated as the mean of the values obtained from the various views.

Measurement of coronary blood flow velocity by Doppler flow wire

After routine left ventriculography and coronary angiography, a 5Fr Judkins guiding catheter (JL, 2.0–3.5 cm) was advanced to the ostium of the coronary artery after administration of 50–100 U/kg heparin. To measure coronary blood flow velocity, we used a 0.014-in-diameter flexible angioplastic guide wire with a 15 MHz piezoelectric ultrasound transducer mounted in its tip (FloWire XT, Cardiometrics, CA, USA). The Doppler flow guide-wire was maintained in the target coronary artery, and was carefully manipulated to obtain the maximum amplitude. Doppler audio signals were processed with a real-time spectrum analyzer using on-line fast Fourier transformation to provide a scrolling gray-scale spectral display. The coronary flow-velocity spectrum envelope was digitized off-line with a

PC/AT computer and a custom-designed software program interfaced with a digitizing tablet. Digitized spectral waveforms from five cardiac cycles were averaged to compute several parameters of intra-coronary flow velocity, including instantaneous spectral peak velocity and time-averaged spectral peak velocity. We measured average peak velocity (APV) at the normal-appearing vessels, at the middle of the aneurysm, at the adjacent normal-appearing vessels approximately 5–10 mm proximal to the aneurysm border, and/or at the inner site of left anterior descending branch (LAD) about 2–3 mm distal from the top of LAD, and left circumflex branch (LCX) confirmed the sensor position with a little bit of angiographic-dye through the guiding catheter (Fig. 1).

Moreover, coronary flow patterns were defined and grouped by two types such as pulsatile flow pattern and disturbed flow pattern at each sampling site. Also, we calculated peak diastolic and systolic flow velocity ratio at the same site.

Intravascular ultrasonography

A 6F sheath was inserted into the right or left femoral artery, and a 6F left guiding catheter was positioned at the coronary ostium. An ultrasound 2.8F imaging catheter with a 20 MHz transducer and a frame rate of 10 per second (EndoSonics, XXX) was advanced down the coronary artery over the 0.014 inch Doppler flow guide-wire. The location of the tip of the intravascular ultrasonography catheter was confirmed by fluoroscopy. Intravascular ultrasonography images were recorded on compact disc, and presence of thrombus (wall adhesive type and free float type) and the diameter and character of the coronary arteries were determined (Fig. 2).

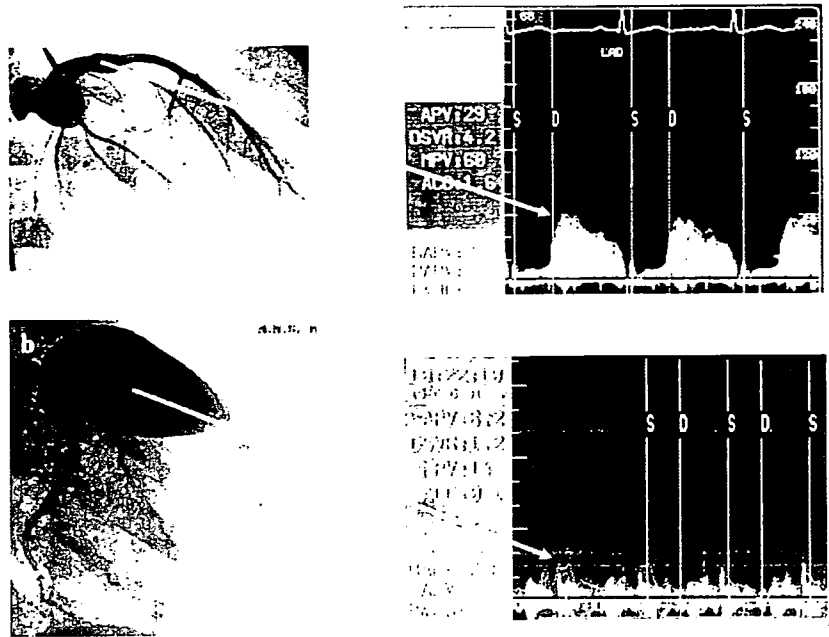
Calculation of shear stress

Blood in all but the smallest vessels (<500 μ m) at all but the lowest shear rates (<200/s) can be treated as an homogeneous Newtonian fluid.⁶ For Newtonian, one-directional flow in a cylindrical tube, the shear rate is equal to the velocity gradient, and the shear stress is the frictional force acting on a unit area of the tube wall and equal to the product of shear rate and the viscosity (μ): Shear stress = $\mu 4Q/\pi R^3$

At shear rates higher than 200/s, the blood viscosity asymptotically approaches a constant value of about 3 cp (cp = 0.003 Pa · s; 1 Pa = 10 dyn/cm²).⁷ For fully developed Poissuille laminar flow, the shear stress at the wall of the tube is related to the volume flow (Q) and half the radius (R). This formula can be simplified as follows: Shear stress = $(4 \times \mu \times APV)/R$.

In this calculation, APV was measured and calculated using a Doppler flow wire, and R was the radius of the coronary artery that was estimated from coronary angiography and intravascular ultrasonography images.

Fig. 1 Measurement of coronary blood flow velocity by Doppler flow wire and calculation of shear stress in (a) small aneurysm and (b) giant aneurysm. (a) Averaged peak flow velocity (APV) was measured in small aneurysm (group A). Shear stress (43.5 dyne/cm^2) was calculated from APV (29 cm/s) and diameter of the coronary vessel (4.8 mm). (b) APV (6.2 cm/s) and shear stress (2.4 dyne/cm^2) were significantly decreased in giant aneurysm (group G). Moreover, coronary flow pattern was disturbed flow pattern.



Patient classification

The subjects were divided into three groups according to presence of coronary artery aneurysm and maximum diameter of coronary artery aneurysm, based on findings of coronary angiography and intravascular ultrasonography. The giant aneurysms group, in which the maximal diameter of coronary artery aneurysms was $>8 \text{ mm}$, was designated as group G, and contained 28 patients. The aneurysms group, in which the maximal diameter of coronary artery aneurysms was $<8 \text{ mm}$,

was designated as group A, and contained 44 patients. The normal appearance group, in which patients had coronary artery aneurysms at the acute stage of Kawasaki disease by 2-D echocardiography, but whose coronary arteries appeared normal on coronary angiography and intravascular ultrasonography images, was designated as group N, and contained 39 patients. Also, the 21 patients in group N for whom we measured and calculated APV and shear stress at the branching site of LAD and LCX were designated as group B (Table 1). Patients with diffuse dilation of coronary artery were not

Fig. 2 Measurement of coronary blood flow velocity by Doppler flow wire and calculation of shear stress at (a) normal-appearing vessels and (b) branching sites. (a) Averaged peak flow velocity (APV) was measured at normal-appearing vessels (group C). Shear stress (38.4 dyne/cm^2) was calculated from APV (16 cm/s) and diameter of the coronary vessel (2.1 mm). (b) APV (6.3 cm/s) and shear stress (9.1 dyne/cm^2) were significantly decreased at about 5 mm distal from the top of the left anterior descending artery and left circumflex artery (segment 5-6-11; group C).

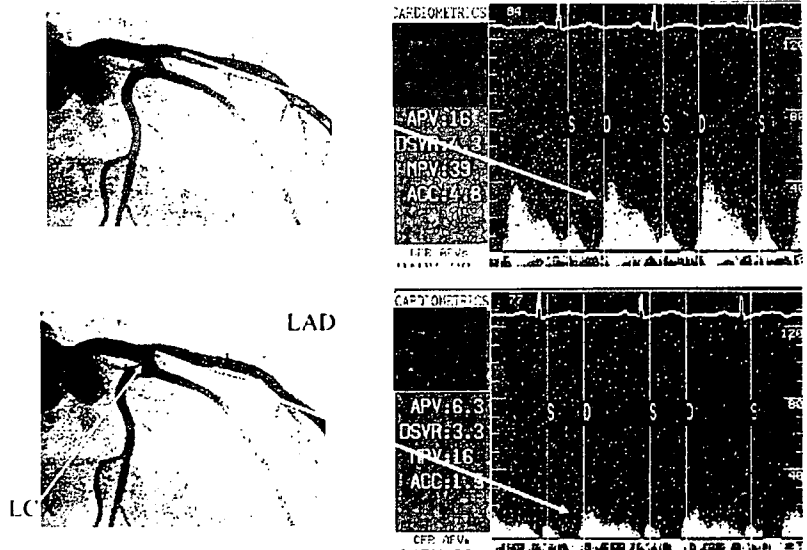


Table 1 Characteristics of subjects

Group	n	Current age	Time from onset to the test	Frequency of patients taking Warfarin
Group G	28	44 ± 27 months	30 ± 19 months	100% (28/28)
Group A	44	47 ± 37 months	37 ± 26 months	18.2% (8/44)
Group N	39	49 ± 34 months	34 ± 21 months	0% (0/0)
Group B	21	98 ± 40 months	49 ± 22 months	0% (0/0)

included in this study. In groups A and G, APV was recorded at the middle of the aneurysm. In group B, APV was recorded at the inner site of LAD about 2–3 mm distal from the top of LAD and LCX. In groups N and A, APV was recorded at the normal-appearing coronary vessels or adjacent normal-appearing vessels approximately 5–10 mm proximal to the aneurysmal border.

Informed consent was obtained from patients or their parents after the study and/or treatment were explained fully.

Statistics

All data are reported as the mean ± standard deviation. Results were analyzed by anova, using Scheffe's method. Differences among three or four groups were considered statistically significant when the value of *P* was <0.05.

Results

Localization of aneurysms by coronary angiography and intravascular ultrasonography

We determined the frequencies at which coronary artery aneurysms localized at the sites examined by coronary angiography and intravascular ultrasonography images. In group G, all 28 aneurysms occurred at major coronary branching sites: 24 occurred at the branching site of the LAD and LCX, and four occurred at the branching site of the first diagonal branch (D_1) and LAD. In group A, 37 of the 44 aneurysms occurred at major coronary branching sites: 33 occurred at the branching site of LAD and LCX, and four occurred at branching site of LAD and D_1 . In contrast, seven aneurysms occurred at non-branching sites of LAD-LCX or LAD- D_1 . Therefore, the majority of the coronary aneurysms we examined occurred at the major branching site of the LAD or LCX, and the giant aneurysms were especially likely to occur at those branching sites (Table 2).

Average peak velocity and shear stress

Using the Doppler flow guide-wire, we were able to stably measure APV in the aneurysms, at the normal-appearing

coronary vessels, at the adjacent normal-appearing vessels to the aneurysmal border, and at the branching sites of the LAD and LCX. APV and shear stress at the normal-appearing vessels (including APV and shear stress at the adjacent normal-appearing coronary vessels to the aneurysmal border) were measured and calculated in all of the 39 patients in group N, and 18 of the 44 patients in group A. In group A, 26 of the 44 coronary artery aneurysmal border existed near the orifice of left coronary artery and APV could not be measured. There were no significant differences among the two groups in APV or shear stress in the normal-appearing vessels and at the adjacent normal-appearing vessels to the aneurysmal border. APV and shear stress values at the giant aneurysms of group G (APV, 7.1 ± 2.1 cm/s; shear stress, 3.8 ± 2.1 dyne/cm²) and at branching sites of the LAD and LCX in group B (APV, 9.1 ± 1.2 cm/s; shear stress, 16.2 ± 3.0 dyne/cm²) were lower than those at the non-giant aneurysms of group A (APV, 21.2 ± 2.6 cm/s; shear stress, 33.2 ± 5.5 dyne/cm²), and at the normal-appearing vessels in groups A and N (APV, 19.6 ± 2.1 cm/s; shear stress, 48.4 ± 5.2 dyne/cm²). Moreover, there were significant differences in APV and shear stress between giant aneurysms and branching sites. In contrast, values of APV and shear stress in normal appearing vessels and non-giant aneurysm group could not find significant differences. Because, the diameter of coronary artery aneurysms were less than 5 mm in almost all cases of non-giant aneurysm group. Therefore, shear stress in giant aneurysms and at branching sites were significantly lower than in non-giant aneurysms, normal-appearing vessels and adjacent normal-appearing vessels to the aneurysmal border, due to reduced coronary flow velocity and increased coronary diameter (Figs 3,4).

Table 2 Frequency and localization of aneurysms detected by coronary angiography and intravascular ultrasonography

Group	Branching site (total)	Branching site of LAD and LCX	Branching site of LAD and D_1
Group G	28/28 (100%)	24/28 (85.7%)	4/28 (14.3%)
Group A	37/44 (84.1%)	33/44 (75.0%)	4/44 (9.1%)
Group N	0/39 (0%)	0/39 (0%)	0/39 (0%)

D_1 , first diagonal artery; LAD, left anterior descending artery; LCX, left circumflex artery.

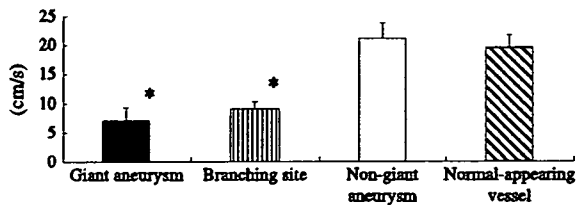


Fig. 3 Averaged peak flow velocity in different situations. * $P < 0.05$ versus other groups.

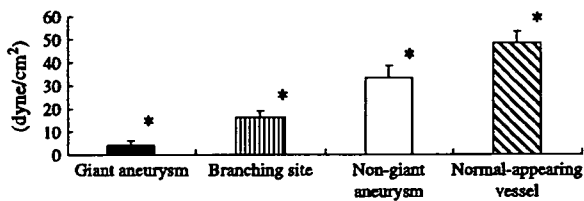


Fig. 4 Shear stress in different situations. * $P < 0.05$ versus other groups.

Coronary flow patterns and peak diastolic and systolic flow velocity ratio

We determined flow patterns under different conditions in coronary artery. In the giant coronary artery aneurysm group, all patients had disturbed flow pattern, and 16 of the 21 patients whose APV at coronary branching sites we were able to measure had disturbed flow pattern; the other patients had pulsatile flow pattern. Moreover, we calculated peak diastolic and systolic flow velocity ratio, it was significantly increase in group G (1.05 ± 0.22) and in group B (4.38 ± 0.85) as compared to that in group A (4.32 ± 0.69) and group N (1.13 ± 0.23 ; $P < 0.01$).

Detection of thrombosis in aneurysms

We determined the frequency of thrombosis in coronary aneurysms. In group G, 24 patients had thrombosis in their coronary

artery aneurysm: 20 had thrombosis of wall adhesive type, and four had thrombosis of free float type (Fig. 5). In contrast, no thrombosis was detected in groups A and N (Table 3). The four patients with free floating type thrombosis underwent urgent coronary artery bypass grafting after percutaneous transluminal coronary revascularization with tissue-type plasminogen activator.

In group G, there were no statistically significant differences in results of thrombotest (TT) or international ratio of prothrombin time (PT/INR) among patients with no thrombosis, wall adhesive type and free float type.

Discussion

In this study, 90.3% of coronary artery aneurysms localized at major coronary branching sites in left coronary artery, and 100% of giant coronary artery aneurysm localized at major branching site of LAD and LCX or LAD and D_1 . Suzuki *et al.*⁸ reported that about 90% of coronary artery aneurysms appeared at coronary branching sites of LAD and LCX, and LAD and D_1 . Their data are consistent with our present findings. Next, we examined the biochemical mechanism by which coronary aneurysm occurs at coronary artery branching sites. We calculated shear stress under different conditions in coronary artery. Both APV and shear stress were significantly lower in giant coronary artery aneurysm and at branching sites of LAD and LCX than in non-giant coronary artery or at normal-appearing coronary vessels. Moreover, all of the flow patterns in the giant coronary artery aneurysm group and three quarters of the flow patterns at LAD and LCX branching sites were disturbed flow patterns. Decreased shear stress and disturbed flow pattern affected coronary artery aneurysm formation.

We previously reported that plasma concentration of monocyte chemoattracted protein-1 (MCP-1) and expression of the *MCP-1* gene by monocytes are significantly increased in the acute stage of Kawasaki disease.⁹ MCP-1 is a novel C-C chemokine that attracts and activates monocytes.¹⁰ Also, we have reported that adhesion of monocytes to endothelial cells is significantly increased in the acute stage of Kawasaki disease.¹¹

Fig. 5 (a) Free-floating thrombosis in giant aneurysm on (b) intravascular ultrasonography.

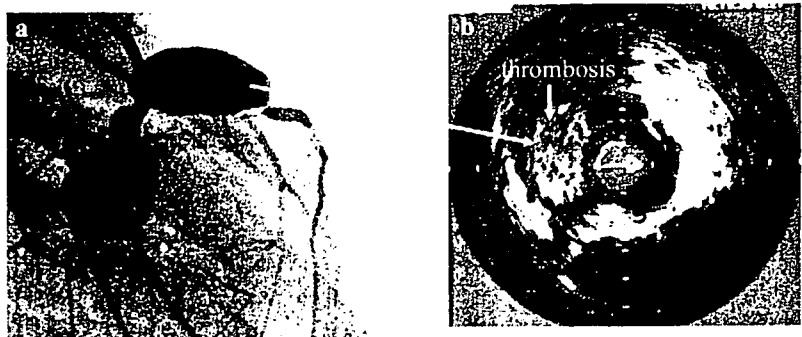


Table 3 Frequency and characteristics of thrombosis in aneurysms

Group	Frequenc	Wall adhesive type	Free floating type
Group G	24/28 (85.75)	20/24 (83.3%)	4/24 (16.7%)
Group A	0/44 (0%)	0/44 (0%)	0/44 (0%)
Group N	0/39 (0%)	0/39 (0%)	0/39 (0%)

Especially, it increases in low shear stress.¹² Then, we speculate that adhered monocyte to endothelial cells could be transmigrated to sub-endothelial space between the endothelial cells and changed the form and character to macrophage. Finally, transmigrated macrophage may destruct extra-matrix of cells and inner-bands and outer-bands, and coronary artery aneurysm may occur. These biochemical and biomechanical findings suggest that coronary artery aneurysms occur at major coronary branching sites of LAD and LCX or LAD and D₁ because of reduced intra-coronary shear stress and disturbed flow pattern. It has been reported that, in adults, atherosclerosis initially occurs at coronary branching and bending sites, where shear stress is relatively low, and low shear rates allow more time for lipoproteins to enter the intima, and for adhesion of white blood cells.^{3,4} The localization of atherosclerotic lesions to arterial geometries associated with disturbed flow patterns suggests an important role for local hemodynamic forces in atherogenesis.⁴ In both these previous studies and the present study, abnormal biomechanical forces affected both atherogenesis and coronary artery aneurysm formation at coronary branching sites.

In the present study, we found a strong negative correlation between frequency of thrombus formation in coronary artery aneurysm and both average peak velocity and shear stress, and a strong positive correlation between the size of coronary artery aneurysm and the frequency of thrombus formation. Many previous studies have found that shear stress affects thrombus formation. Decreased shear stress leads to reduced production of prostaglandin₂¹³ and nitric oxide,¹⁴ resulting in increased platelet aggregation. Decreased shear stress also increases endothelial cell tissue factor activity¹⁵ and levels of human protease-activated receptor-1 mRNA,¹⁶ and reduces thrombomodulin expression,¹⁷ resulting in elevated coagulation. Simultaneously, decreased shear stress induces reduction of fibrinolysis by reducing production of tissue plasminogen activator^{16,18} and increasing production of plasminogen activator inhibitor-1. Such a combination of elevated platelet aggregation and coagulation and reduced fibrinolysis would clearly promote thrombogenicity. Moreover, in the present study, disturbed flow pattern also greatly affected thrombus formation. In the present subjects, TT and PT/INR were maintained at acceptable values. However, almost all cases in the giant aneurysm group exhibited thrombus formation in the coronary artery aneu-

rysm. This indicates that ordinary anticoagulant therapy has limited effect in patients with such greatly reduced shear stress and abnormal flow pattern. We performed urgent coronary artery bypass graft in four patients with free floating type thrombosis in giant coronary aneurysm, to prevent acute myocardial infarction.

In the present study, we did not test the right coronary artery. In our experience, all right coronary artery aneurysms occur at the bending sites in segment I. However, it is somewhat difficult to measure APV at bending sites of the right coronary artery. It has been reported that shear stress in the coronary artery decreases at the bending site.⁴ The mechanisms involved in left coronary artery aneurysm formation may affect right coronary artery aneurysm formation.

Study limitations

There are methodological problems associated with measurement of blood flow velocity using a Doppler guide-wire.¹⁹⁻²¹ Some studies have found that a Doppler system can accurately measure flow velocity in a straight tube model, but those studies were performed under non-physiological conditions. Flow velocity may be underestimated in small-diameter vessels, due to inability to position the wire tip far enough from the wall to sample the central portion of the stream. Also, flow velocity tends to be underestimated in tightly curved regions of a tortuous vessel. These methodological limitations should be taken into consideration when analyzing results obtained using a Doppler guide-wire.

Conclusions

In patients with Kawasaki disease, coronary artery aneurysms predominantly localize at major coronary artery branching sites, in a manner similar to that in which atherosclerosis in adults initially forms at branching sites. Stagnation of coronary flow velocity, reduced shear stress and disturbed flow pattern may appear to play a critical role in coronary artery aneurysm and thrombus formation in children with Kawasaki disease.

References

- 1 Fujiwara H, Hamashima Y. Pathology of the heart in Kawasaki disease. *Pediatrics* 1978; 61: 100-107.
- 2 Kato F, Ichinose E, Kawasaki T. Myocardial infarction in Kawasaki disease: clinical analysis in 195 cases. *J. Pediatr.* 1986; 108: 923-7.
- 3 Asakura T, Karino T. Flow patterns and spatial distribution of atherosclerotic lesions I human coronary arteries. *Circ. Res.* 1990; 66: 1045-66.